

Chemistry—A European Journal

Supporting Information

Directed Gas Phase Formation of Silene (H_2SiCH_2)

Zhenghai Yang,^[a] Srinivas Doddipatla,^[a] Chao He,^[a] Vladislav S. Krasnoukhov,^[b] Valeriy N. Azyazov,^[b, c] Alexander M. Mebel,*^[d] and Ralf I. Kaiser*^[a]

EXPERIMENTAL & COMPUTATIONAL

Experimental Section

The bimolecular reaction of methylidyne (CH , $\text{X}^2\Pi$) with silane (SiH_4) was performed under single collision conditions in a crossed molecular beam machine at the University of Hawaii.^[1] The pulsed supersonic methylidyne beam was produced via photodissociation (COMPex 110, Coherent, Inc.; 248 nm; 30 Hz) of helium-seeded (99.9999%; AirGas) bromoform (CHBr_3 , Sigma-Aldrich, $\geq 99\%$) held in a stainless steel bubbler at 283 K at a total pressure of 2.2 atm.^[2] After passing through the skimmer, the methylidyne beam was velocity selected by a four-slot chopper wheel with a peak velocity of $v_p = 1846 \pm 12 \text{ m s}^{-1}$ and a speed ratio S of 13.5 ± 0.6 (Table S1). Using laser-induced fluorescence, the methylidyne radical beam was characterized by a rotational temperature of $14 \pm 1 \text{ K}$.^[3] The supersonic beam of neat silane (Linde, 99.999%) at a backing pressure of 550 Torr with a peak velocity of $v_p = 827 \pm 20 \text{ m s}^{-1}$ and a speed ratio S of 10.1 ± 0.2 (Table S1) crossed perpendicularly with the methylidyne beam, resulting in a collision energy of $18.9 \pm 0.1 \text{ kJ mol}^{-1}$ and a center-of mass angle Θ_{CM} of $48.5 \pm 0.2^\circ$. Each supersonic beam initiated in a piezoelectric pulse valve, which was operated at a repetition rate of 60 Hz, a pulse width of 80 μs , and a peak voltage of -400 V. The secondary pulse valve was triggered 76 μs prior to the primary pulse valve, introducing the pure silane gas. The detector is housed within a triply differentially pumped chamber and rotatable in the plane defined by both reactant beams. It comprises a Brink-type ionizer,^[4] a quadrupole mass spectrometer (QMS), and a Daly-type ion counter.^[5] The neutral reaction products entering the detector were ionized by electron impact (80 eV), filtered based on their mass-to-charge ratios (m/z) utilizing a QMS (Extrel; QC 150) equipped with a 1.2 MHz oscillator, and eventually recorded by a Daly-type ion counter. Based on user-defined center-of mass (CM) translational energy $P(E_T)$ and angular $T(\theta)$ flux distributions, a forward convolution routine was used to analyze the laboratory data. These functions, which define the reactive differential cross section $I(u, \theta) \sim P(u) \times T(\theta)$ with the center-of-mass velocity u , are varied until an acceptable fit of the laboratory frame (LAB) TOF spectra and angular distributions is obtained.^[6] The error ranges of the $P(E_T)$ and $T(\theta)$ functions are determined within 1σ limits of the corresponding laboratory angular distribution while maintaining a good fit of the laboratory TOF spectra.

Computational Section

Geometry optimization of the reactants, products, intermediates, and transition states involved in the CH + SiH₄ reaction was carried out using the doubly hybrid DFT B2PLYPD3 method^[7] with Dunning's correlation-consistent cc-pVTZ basis set.^[8] Vibrational frequencies and zero-point vibrational energy corrections (ZPE) were computed at the same B2PLYPD3/cc-pVTZ level of theory. Next, single-point energies of the optimized structures were recalculated at the explicitly correlated coupled clusters CCSD(T)-F12/cc-pVQZ-f12 level of theory,^[9] which closely approximates CCSD(T)/CBS energies, i.e. the energies within the coupled clusters theory with single and double excitations with perturbative treatment of triple excitations in the complete basis set limit. The anticipated accuracy of the CCSD(T)-F12/cc-pVQZ-f12//B2PLYPD3/cc-pVTZ + ZPE(B2PLYPD3/cc-pVTZ) relative energies is better than within 4 kJ mol⁻¹.^[10] B2PLYPD3 and CCSD(T)-F12 calculations were performed using the Gaussian 09^[11] and Molpro 2010^[12] software package, respectively. Rice-Ramsperger-Kassel-Marcus (RRKM) theory,^[13] was employed to compute energy-dependent rate constants of all unimolecular reaction steps on the CSiH₅ PES ensuing the initial insertion of the CH radical into a Si-H bond forming **i1**. Internal energy dependent rate constants were calculated within the harmonic approximation using B2PLYPD3/cc-pVTZ frequencies with our in-house code Unimol.^[14] Unimol automatically processes GAUSSIAN 09 log files and evaluates numbers of states for transition states and densities of states for local minima with the use of the direct count method. The internal energy was assumed to be equal to the sum of the collision energy and the chemical activation energy, that is, negative of the relative energy of a species with respect to the reactants. Only one energy level was considered throughout as at a zero-pressure limit corresponding to crossed molecular beams conditions. For the H loss channels forming **p1** and **p3** without exit barriers, rate constants were computed using microcanonical variational transition state theory (VTST).^[13, 15] Here, to determine the minimal value of the H elimination rate constant $k(E)$ for a particular channel, the minimal potential energy profile (MEP) was scanned along the breaking Si-H or C-H bond. The MEP structures were obtained via partial B2PLYPD3/cc-pVTZ geometry optimization with fixed values of the Si-H or C-H distance with all other geometric parameters being optimized. Then, 3N-7 vibrational frequencies were computed projecting the reaction coordinate out and single-point energies along the MEP were refined at the CCSD(T)-F12/cc-pVQZ-f12 level. RRKM and VTST rate constants were then

utilized to compute product branching ratios by solving first-order kinetic equations within steady-state approximation.^[14-15] The branching ratios are presented in Table S2.

Table S1. Peak Velocity (v_p) and Speed Ratios (S) of the Methylidyne (CH) and Silane (SiH_4) Beams along with the Corresponding Collision Energy (E_c) and Center-of-Mass Angle Θ_{CM} .

beam	v_p (m s $^{-1}$)	S	E_c (kJ mol $^{-1}$)	Θ_{CM} (deg)
CH	1846 ± 12	13.5 ± 0.6		
SiH_4	827 ± 20	10.1 ± 0.2	18.9 ± 0.1	48.5 ± 0.2

Table S2. Product branching ratios calculated at a collision energy of 18.9 kJmol $^{-1}$.

Product	p1 total	p1 from i1	p1 from i2	p2	p3	p4	p5	p6	p7
Branching Ratio (%)	96.127	78.510	17.617	3.865	0	0	0.008	0	0

Table S3. Cartesian coordinates and frequencies (cm^{-1}) of reactants, intermediates, transition states, and products. Point groups and ground electronic wave functions are also included.

Reactants

SiH₄, T_d, ¹A₁

Si	0.000000	0.000000	0.000070
H	0.000000	0.000000	-1.478347
H	0.000000	1.393917	0.492458
H	-1.207168	-0.696959	0.492458
H	1.207168	-0.696959	0.492458

Frequencies

944.8900	945.3209	945.3219
996.7993	996.8018	2280.5787
2286.0806	2286.5567	2286.5734

CH, C_{∞v}, ²Π

C	0.000000	0.000000	0.159796
H	0.000000	0.000000	-0.958776

Frequencies

2874.2918

Products

p1, C_{2v}, ¹A₁

Si	-0.9470952407	-0.2901881419	-0.3157726295
C	0.4443044414	-0.4150863201	0.6678149884
H	-1.6604997633	0.9798858066	-0.5273447377
H	-1.5294620662	-1.4440974627	-1.0201436692
H	0.8625447925	0.439387053	1.1799120895
H	0.9591018362	-1.3534809348	0.8151669583

Frequencies

463.4611	479.2241	737.1532
777.3567	836.9079	942.4408
995.5029	1405.7596	2290.2322
2310.7575	3166.1462	3257.8693

p2 (singlet), C_s, ¹A'

Si	-0.8712493169	0.2012834616	-0.5112756599
C	1.0145745734	0.1893731305	-0.2975501988
H	-1.07911341	-1.1476558149	0.1596479906
H	1.4346196952	-0.6972441437	-0.7809264756
H	1.5036203263	1.0736121164	-0.697022984
H	1.2641901319	0.0942542501	0.7630303276

Frequencies

140.8407	564.5817	631.1110
673.1402	954.1628	1261.3452
1443.4641	1460.2304	2044.2249
3015.9636	3076.1306	3136.2455

p2 (triplet), C_s, ³A”

Si	0.719279	-0.116234	0.000010
C	-1.164391	0.047697	0.000009
H	1.541460	1.118582	-0.000056
H	-1.501341	0.579496	-0.888013
H	-1.622311	-0.938567	0.001118
H	-1.501367	0.581587	0.886755

Frequencies

125.7661	559.7736	677.9973
792.2706	883.1074	1272.2603
1463.3294	1463.8317	2198.8796
3046.6264	3125.7564	3140.0191

p3 (triplet), C_s, ³A”

Si	0.507332	0.008483	0.000002
C	-1.309298	-0.087592	0.000010
H	1.066243	-1.361644	-0.004798
H	0.995812	0.719928	1.206896
H	0.995214	0.728160	-1.202250
H	-2.304128	0.320340	0.000072

Frequencies

115.3978	367.7162	641.9158
654.1048	804.8058	957.0915
959.5761	959.6632	2228.5270
2230.8463	2255.3028	3288.1957

p3 (singlet), C₁, ¹A

Si	-0.84551	0.00489	-0.4712
C	1.1069	0.18216	-0.50447
H	-1.51873	1.25262	-1.03406
H	-1.01275	-0.01365	1.06015
H	-1.49825	-1.25262	-1.06015
H	1.51873	-0.8429	-0.50203

Frequencies

344.7536	453.3581	620.4371
639.6613	887.3134	942.1262
950.9926	1014.5933	1965.2977
1988.6248	2039.2851	2996.1181

p4, C_s, ²A''

Si	-0.792669	-0.000003	-0.004689
C	1.102754	-0.000010	-0.014242
H	1.554719	-0.890644	-0.450164
H	1.554650	0.890417	-0.450666
H	1.371473	0.000327	1.051931

Frequencies

517.9764	612.7681	679.8678
1254.2770	1370.5974	1454.0473
2984.9286	3072.0088	3109.2042

p5, C_s, ²A'

Si	-0.59906	-0.1196	0.0
C	1.09536	0.05669	0.0
H	-1.50903	1.06206	0.0
H	1.78524	-0.77695	0.0
H	1.53846	1.04918	0.0

Frequencies

282.8783	523.6148	778.9553
843.0915	1050.8640	1382.3569
2165.3493	3117.3241	3225.4890

p6, C_{2v}, ²B₂

Si	0.484127	-0.000004	-0.000007
C	-1.181849	0.000031	-0.000001
H	1.283233	-1.236120	0.000041
H	1.283252	1.236099	0.000041
H	-2.253174	-0.000110	0.000029

Frequencies

245.3542	394.9789	606.3356
713.5392	960.8485	1143.6050
2285.4214	2294.8623	3344.8565

p7, Cs, 2A”

Si	0.437938	0.000041	0.004673
C	-1.475226	0.000240	0.046409
H	0.567932	-0.009159	-1.480063
H	1.076401	-1.208582	0.575389
H	1.075888	1.215734	0.560796

Frequencies

305.4785	459.3822	684.6607
889.9670	903.2367	966.3571
2201.9026	2243.2445	2248.2777

Intermediates**i1, Cs, 2A'**

Si	-0.645087408	-0.0440451562	-0.115805493
C	1.0826856242	0.0109244033	-0.7703379996
H	-1.3237973352	-1.2803033725	-0.5683342733
H	-1.4094058916	1.1364136065	-0.5823319957
H	-0.6604361015	-0.0344622424	1.3698618179
H	1.6571284849	-0.882836615	-0.9707552981
H	1.6115296272	0.9381973763	-0.9423887581

Frequencies

30.6549	527.3099	527.5688
672.8621	757.9876	850.9093
958.6206	961.0159	972.2380
1419.6605	2218.2697	2248.0167
2252.2624	3155.2202	3249.1910

i2, Cs, 2A'

Si	-0.5891129945	-0.246419088	-0.3185174015
C	0.8991056286	-0.372322082	0.8321214217
H	-1.2185066861	1.097767061	-0.2535473451
H	-1.6076142356	-1.2833335013	-0.0108530283
H	1.3636875899	-1.3539108561	0.7591462504
H	1.6467414824	0.3783043848	0.582561491
H	0.5941622154	-0.2168779184	1.8681326119

Frequencies

183.9484	530.0073	576.7677
694.7207	855.5745	894.9155
946.7104	1291.4668	1468.6119
1472.4543	2206.6347	2229.3904
3047.2530	3122.8206	3142.6962

Transition states**i1-i2, C_s, 2A'**

Si -0.9284442756 -0.2097711206 -0.3045569178
 C 0.9024581269 -0.2509499368 -0.195619257
 H -1.5401144826 -1.2525672355 -1.1535517082
 H -1.5281373381 1.1320756665 -0.4534608586
 H -0.0788150995 -0.5885726898 0.971170015
 H 1.4508748015 -1.1735609429 -0.3225219259
 H 1.4597272674 0.5887252591 0.1948586524

Frequencies

1792.6356 <i>i</i>	294.6471	530.0393
606.1062	670.7597	787.0389
824.8794	905.9269	1019.7694
1384.5890	1916.2077	2237.6330
2272.7026	3156.9017	3260.9272

i1-p1, C_s, 2A'

Si 0.8258435997 -0.0045375108 -0.8526374438
 C -0.7481514929 -0.0228752223 -0.1992613949
 H 1.5642361805 1.2412616895 -1.1145563732
 H 1.5691942024 -1.2338572073 -1.1720797857
 H 0.8210338465 -0.0749364862 2.1765261298
 H -1.2791809201 0.8867396153 0.0407952496
 H -1.275512416 -0.9447788782 -0.0017703819

189.8701 <i>i</i>	62.8264	114.4906
480.8417	505.4762	746.0437
798.0425	838.2521	948.3657
1051.0161	1412.5531	2293.0884
2313.8864	3169.3362	3261.0726

i1-p6, C₁, 2A

Si -0.53727 -0.071 -0.02517
 C 1.27248 -0.0824 0.03951
 H -1.26832 -1.28291 -0.51326
 H -1.14947 0.32185 1.26474
 H 2.19391 -0.64857 0.06103
 H -0.39088 1.44918 -0.59118
 H 0.50169 1.64885 -0.10596

Frequencies

1473.7421 <i>i</i>	286.3688	535.4156
579.8428	631.2850	730.3959
824.5770	903.8582	1018.3502

1047.0775	1744.4907	2144.3384
2238.9401	3149.7625	3378.8415

i1-p7, C₁, ²A

Si -1.18378	-0.34804	-0.16697
C 0.71422	-0.94573	-0.11885
H -1.83981	-0.49337	1.20791
H -1.98763	-1.13041	-1.20791
H -1.12449	1.13041	-0.56037
H 1.98763	0.25131	-0.56264
H 1.69053	0.92539	0.12618

Frequencies

1046.4844 <i>i</i>	266.7138	461.5379
568.0938	617.8292	655.3894
954.2363	970.2694	997.3834
1304.1876	1426.5894	1712.3756
2000.6047	2011.1094	2014.8431

i2-p1, C_s, ²A'

Si -0.7113453898	-0.0115003109	-0.0068192203
C 0.9942222404	0.0736614199	0.0201931216
H -1.5395021061	0.9064368734	-0.8046663672
H -1.4664048019	-1.0418269831	0.7234631742
H 1.5943308868	-1.3032188284	-1.7661987168
H 1.5370355639	0.8426970089	-0.509283445
H 1.5910306069	-0.5974481797	0.6200634535

Frequencies

331.4416 <i>i</i>	172.6973	196.4863
482.5824	513.9522	760.2708
806.5857	840.8712	946.3245
1037.6937	1409.8010	2294.7908
2316.6164	3171.7978	3264.2480

i2-p5, C₁, ²A

Si -0.64086	-0.00026	-0.029
C 1.12016	-0.19288	0.00322
H -1.53315	-1.18501	0.3401
H 1.65285	-1.0819	-0.33414
H 1.74558	0.4701	0.5928
H 0.59074	1.32096	-0.35985
H -0.20499	1.63674	0.14774

Frequencies

1672.4204 <i>i</i>	273.4788	595.1074
--------------------	----------	----------

749.8826	783.7070	865.8321
976.0561	1003.8783	1209.5522
1401.3794	1461.3420	1820.6714
1937.8334	3088.1295	3174.8807

p1-p2, C₁, ¹A

Si	-0.661626	-0.074776	-0.083054
C	1.128647	0.073328	-0.043223
H	-1.062088	1.282517	0.422267
H	0.093567	-0.802561	1.077027
H	1.713770	-0.830383	-0.183917
H	1.745631	0.957321	0.106719

Frequencies

1165.5344 <i>i</i>	586.9428	789.2099
823.1202	896.3444	999.5665
1016.0886	1446.3614	1912.4961
2131.3235	3096.5117	3189.4576

p1-p6, C_s, ²A'

Si	0.667361	0.063830	0.000002
C	-1.025390	-0.388578	-0.000010
H	1.073400	1.524082	-0.000024
H	1.818042	-0.932417	0.000010
H	-1.592545	-1.304532	0.000021
H	-1.963968	0.759549	-0.000031
H	-2.525644	1.391169	0.000049

Frequencies

999.3757 <i>i</i>	257.9749	348.0831
551.5637	632.5875	741.8248
787.4532	795.5619	914.1213
987.6829	1029.5461	2044.6453
2091.1253	2256.4783	3262.6738

p4-p5, C₁, ²A

Si	0.717697	-0.047763	-0.023934
C	-1.089650	-0.065540	-0.037431
H	-0.114810	1.151884	0.609908
H	-1.717774	-0.809229	0.456089
H	-1.677268	0.719269	-0.506329

Frequencies

$1259.9166i$	615.0452	781.1231
926.9542	1034.8934	1416.3675
1795.5382	3063.0444	3154.8679

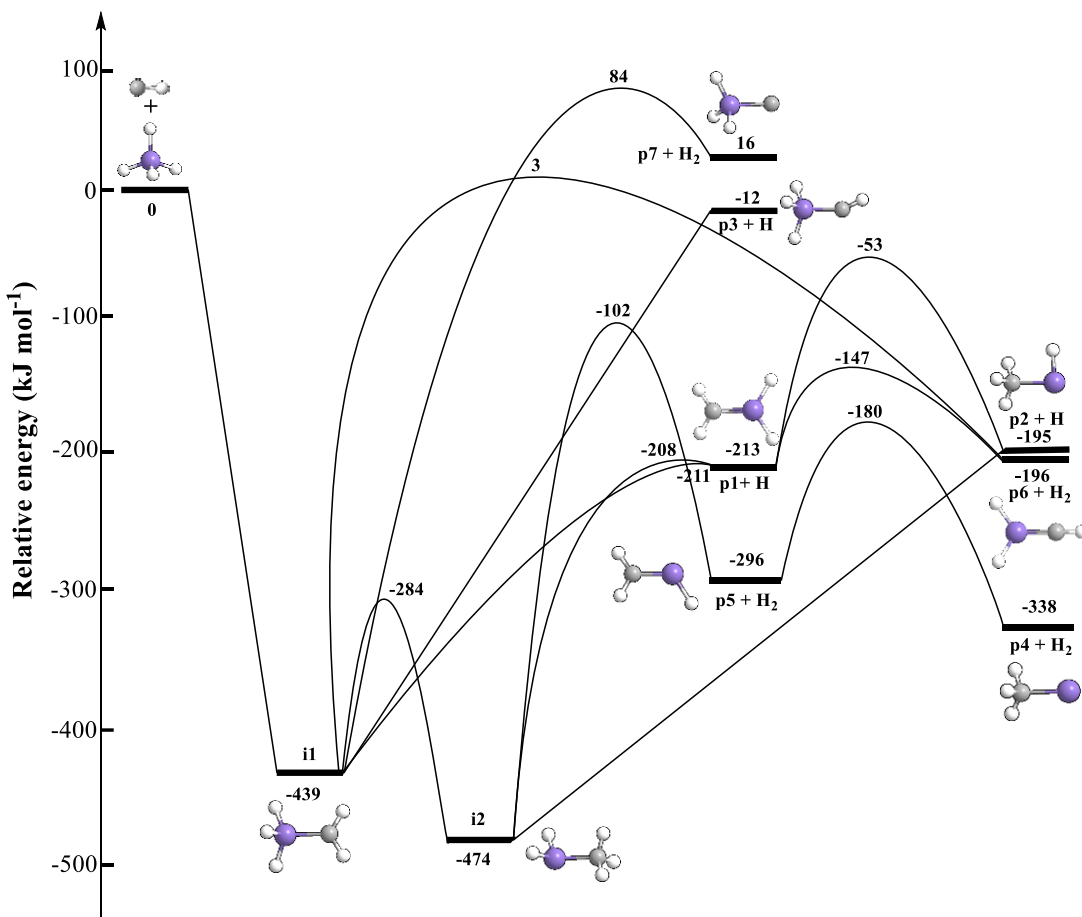


Figure S1. Potential energy surface for the reaction of the methylidyne radical with silane involving atomic and molecular hydrogen loss pathways. Optimized Cartesian coordinates of the atoms and vibrational frequencies are compiled in Table S3. Carbon, silicon, and hydrogen are color coded in gray, purple, and white, respectively.

References

- [1] a) R. I. Kaiser, P. Maksyutenko, C. Ennis, F. Zhang, X. Gu, S. P. Krishtal, A. M. Mebel, O. Kostko, M. Ahmed, *Faraday Discuss.* **2010**, *147*, 429-478; b) X. Gu, Y. Guo, F. Zhang, A. M. Mebel, R. I. Kaiser, *Faraday Discuss.* **2006**, *133*, 245-275.
- [2] a) C. He, A. M. Thomas, G. R. Galimova, A. M. Mebel, R. I. Kaiser, *J. Phys. Chem. A* **2019**, *123*, 10543-10555; b) C. He, A. M. Thomas, G. R. Galimova, A. N. Morozov, A. M. Mebel, R. I. Kaiser, *J. Am. Chem. Soc.* **2020**, *142*, 3205-3213; c) A. M. Thomas, L. Zhao, C. He, G. R. Galimova, A. M. Mebel, R. I. Kaiser, *Angew. Chem. Int. Ed.* **2019**, *58*, 15488-15495.
- [3] a) R. I. Kaiser, X. Gu, F. Zhang, P. Maksyutenko, *Phys.Chem.Chem.Phys.* **2012**, *14*, 575-588; b) P. Maksyutenko, F. Zhang, X. Gu, R. I. Kaiser, *Phys.Chem.Chem.Phys.* **2011**, *13*, 240-252.
- [4] G. O. Brink, *Rev. Sci. Instrum.* **1966**, *37*, 857-860.
- [5] N. Daly, *Rev. Sci. Instrum.* **1960**, *31*, 264-267.
- [6] a) J. D. Bittner, Massachusetts Institute of Technology **1981**; b) P. Weiss, Lawrence Berkeley Lab., CA (USA) **1986**; c) R. I. Kaiser, T. N. Le, T. L. Nguyen, A. M. Mebel, N. Balucani, Y. T. Lee, F. Stahl, P. v. R. Schleyer, H. F. Schaefer III, *Faraday Discuss.* **2002**, *119*, 51-66.
- [7] a) S. Grimme, *J. Chem. Phys.* **2006**, *124*, 034108; b) L. Goerigk, S. Grimme, *J. Chem. Theory Comput.* **2011**, *7*, 291-309; c) S. Grimme, S. Ehrlich, L. Goerigk, *J. Comput. Chem.* **2011**, *32*, 1456-1465.
- [8] T. H. Dunning Jr, *J. Chem. Phys.* **1989**, *90*, 1007-1023.
- [9] a) T. B. Adler, G. Knizia, H.-J. Werner, *J. Chem. Phys.* **2007**, *127*, 221106; b) G. Knizia, T. B. Adler, H.-J. Werner, *J. Chem. Phys.* **2009**, *130*, 054104.
- [10] J. Zhang, E. F. Valeev, *J. Chem. Theory Comput.* **2012**, *8*, 3175-3186.
- [11] M. Frisch, G. Trucks, H. Schlegel, G. Scuseria, M. Robb, J. Cheeseman, G. Scalmani, V. Barone, B. Mennucci, *Gaussian 09 Revision D. 01*, Gaussian, Inc.: Wallingford CT, **2009**.
- [12] H.-J. Werner, P. Knowles, R. Lindh, F. Manby, M. Schütz, P. Celani, T. Korona, A. Mitrushenkov, G. Rauhut, *MOLPRO, version 2010.1, a package of ab initio programs*, University of Cardiff, Cardiff, UK, **2010**.

- [13] a) P. J. Robinson, K. A. Holbrook, **1972**; b) H. Eyring, S. H. Lin, S. M. Lin, *Basic chemical kinetics*, John Wiley & Sons, New York, **1980**; c) J. I. Steinfeld, J. S. Francisco, W. L. Hase, *Chemical kinetics and dynamics, Vol. 3*, Prentice Hall, Englewood Cliffs, **1982**.
- [14] C. He, L. Zhao, A. M. Thomas, A. N. Morozov, A. M. Mebel, R. I. Kaiser, *J. Phys. Chem. A* **2019**, *123*, 5446-5462.
- [15] V. Kislov, T. L. Nguyen, A. Mebel, S. Lin, S. Smith, *J. Chem. Phys.* **2004**, *120*, 7008-7017.